

Six-Photon Amplitudes

T. Binoth, and G. Heinrich,

School of Physics, The University of Edinburgh, Edinburgh EH9 3JZ, Scotland

T. Gehrmann, and P. Mastrolia

Institut für Theoretische Physik, Universität Zürich, CH-8057 Zürich, Switzerland

We derive the six-photon scattering amplitudes for all helicity configurations, obtaining compact analytical expressions. Two recently developed methods, based on form factor decomposition and on multiple cuts are used for this calculation.

The self-interaction of photons (light-by-light scattering) mediated through a virtual charged fermion loop is a fundamental, although yet unobserved, prediction of quantum electrodynamics. The corresponding multi-photon scattering amplitudes are of outstanding theoretical interest, since they exhibit a high degree of symmetry. They can be used to establish and further develop methods for the calculation of virtual corrections to multi-leg processes, and to study symmetry patterns in the results, thus providing further insight into the analytical structure of quantum field theories at the loop level.

In the past, the four-photon amplitudes were derived at one loop for massless and massive fermions [1], and at two loops for massless fermions [2]. At two loops, four-photon scattering in supersymmetric Yang-Mills theories [3] was studied as well, yielding first evidence for a leading transcendentality behaviour, which was uncovered subsequently also in multi-gluon amplitudes [4], and has sparked many new developments (see [5] and references therein) in the study of multi-loop scattering amplitudes in super-Yang-Mills theories and perturbative gravity.

The computation of one-loop multi-particle amplitudes is currently among the most pressing issues in the preparation of precision next-to-leading order (NLO) calculations for the upcoming CERN LHC experiments. Given the large variety of potentially interesting multi-particle final states, automated methods for one-loop corrections would be very desirable, and are currently under intense development [6, 7, 8, 9, 10, 11, 12, 13, 14, 15, 16, 17, 18, 19, 20, 21, 22, 23, 24]. These methods range from purely analytical schemes to completely numerical approaches.

Compact analytical expressions for amplitudes involving $n > 4$ external photons were obtained only for specific helicity configurations. All amplitudes with odd n vanish due to parity conservation; amplitudes with even $n > 4$

vanish if all or all but one photons have the same helicity [25]. For $n = 6$ external photons, one finds therefore only two non-vanishing amplitudes, which we denote by $A_6(++++)$ and $A_6(+-+)$. An analytical expression for $A_6(++++)$ was computed already long ago [26], using the method described in [25]. $A_6(+-+)$ was obtained recently using a purely numerical method for the loop integration. In this paper, we use two completely different recently developed methods (based either on form factor decomposition [6] or on multiple cuts [11, 12, 13, 14]) to compute $A_6(++++)$ and $A_6(+-+)$, obtaining compact results which respect the symmetry properties of the process under consideration. Besides allowing a prediction for the process $gg \rightarrow 4\gamma$, our results serve as a highly non-trivial proof of applicability of both methods used, and illustrate how form factor-based and cut-based techniques can be matched onto each other in detail.

1. Structure of the Amplitudes

Despite the absence of a corresponding tree-level process and the (Feynman) diagram-by-diagram UV-finiteness in four dimensions, the cut-constructibility of the 6-photon amplitudes is not guaranteed, in accordance with the power counting argument in [31]. The fact that the rational parts of the six-photon amplitudes actually do evaluate to zero was shown in [27]. Consequently, the amplitude can be written as a linear combination of poly-logarithms and transcendental constants, associated to a known basis of functions, the master integrals (MI), formed by box-, triangle- and bubble-type integrals [28, 29, 30].

The result for the amplitude $A_6(++++)$ has the

following structure

$$A_6(+ + + +) = \frac{e^6}{(4)^2} \sum_{2S_4=(\mathbb{Z}_2, \mathbb{Z}_2)} X_h F_1(s_{13}; s_{14}; s_{134}) + F_1(s_{23}; s_{24}; s_{234}) + F_{2B}(s_{135}; s_{145}; s_{15}; s_{26})_i + F_{2B}(s_{235}; s_{245}; s_{25}; s_{16})_i ; \quad (1)$$

where

$$F_i = d_i - F_i \quad (i = 1; 2B) :$$

F_1, F_{2B} are the finite parts of the one-mass and two-mass-easy box functions [29, 30], and d_1 and d_{2B} are their coefficients, that can be obtained from (6) and (10) below. The sum in Eq.(1) runs over the discrete quotient group $S_4(3;4;5;6) = (\mathbb{Z}_2(3;4) \times \mathbb{Z}_2(5;6))$ which has 6 elements. The quotient space structure can be inferred from the symmetry properties of the combination of basis functions. It is invariant under interchanging the indices $3 \leftrightarrow 4$ and $5 \leftrightarrow 6$. The permutations generate exactly those functions which are allowed by the cutting rules.

The result for the amplitude $A_6(+ + + +)$ has the following structure

$$A_6(+ + + +) = \frac{e^6}{(4)^2} \sum_{2S_3=(\mathbb{Z}_2, \mathbb{Z}_2)} X_h F_1(s_{12}; s_{23}; s_{456}) + \sum_{2S_3=(\mathbb{Z}_2, \mathbb{Z}_2)} X_h F_1(s_{61}; s_{12}; s_{345}) + \sum_{2S_3=(\mathbb{Z}_2, \mathbb{Z}_2)} X_h F_{2A}(s_{12}; s_{234}; s_{34}; s_{56})_i + \sum_{2S_3} X_h I_3(s_{12}; s_{34}; s_{56})_i ; \quad (2)$$

where

$$F_i = d_i - F_i \quad (i = 1; 2A) ; \text{ and } I_3 = c_3 - I_3 :$$

F_1, F_{2A} are the finite parts of the one-mass and two-mass-hard box functions, I_3 is the triangle function with 3 on-shell legs and d_1, d_{2A} , and c_3 are obtained from (18), (14) and (24) given in section 2. The different permutation groups in (2), i.e. $S_3(1;3;5) = \mathbb{Z}_2(1;3) \times \mathbb{Z}_2(2;4;6) = \mathbb{Z}_2(4;6)$ for the first term, $S_3(1;3;5) = \mathbb{Z}_2(3;5) \times \mathbb{Z}_2(2;4;6) = \mathbb{Z}_2(2;6)$ for the second term, $S_3(1;3;5) \times \mathbb{Z}_2(2;4;6)$ for the third

one and $S_3(2;4;6)$ for the last term, contain 9, 9, 36 and 6 elements respectively. They generate all possible different basis functions F_1, F_{2A} and I_3 which are allowed by cutting rules. Note that each cut is corresponding to a certain Mandelstam variable. Compatibility with cutting rules means that no Mandelstam variables s_{ij} or s_{ijk} appear as a function argument such that the corresponding legs $i; j; k$ have like-sign helicities. This is certainly only true for amplitudes with massless particles.

2. Cut-Construction

As the six-photon amplitudes are cut-constructible, the computational effort is reduced to the computation of the rational coefficients of a linear combination of master integrals as described in section 1. According to the principle of unitarity-based methods [31], the exploitation of the unitarity-cuts of each master integral enables the extraction of the corresponding coefficient from the amplitude. To that aim, we employ the quadruple-cut technique [11] for box-coefficients, the triple-cut integration [14] for triangle-coefficients, and the double-cut integration [12, 13] for bubble-coefficients, by sewing in the multiple cuts the QED tree-level amplitudes given in [32]. Spinor algebra and numerical evaluation of spinor products has been implemented in a Mathematica package [33]. In the following we use by now standard spinor notation, with $\langle a | \mathcal{P}_{i::j} | b \rangle = \langle a | \mathcal{P}_{i::j} | b \rangle$, and multiparticle momenta denoted as $P_{i::j} = p_i + \dots + p_j$, with p_k being the momentum of the k -th external photon, considered incoming.

2.1. Construction of $A_6(+ + + +)$

The analytic expression for $A_6(+ + + +)$ was computed by Mahlon [26]. It can be expressed in terms of the two classes of box functions F_1 and F_{2B} as shown in eq. (1). Using the symmetry of the amplitude, it is sufficient to compute the coefficients of a representative box-function for each of the two classes (and their parity-conjugates).

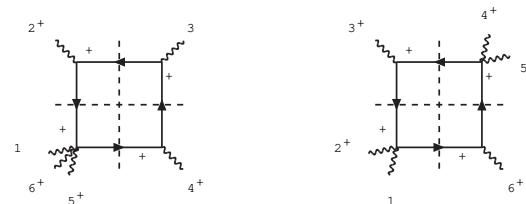


Figure 1. Quadruple-Cuts, $d_1^{(1)}$ (left) and $d_{2B}^{(1)}$ (right). Reverse internal-helicity counterparts understood.

$$r_1 = 8 \frac{S_{23} S_{34}}{h_2^2 4i^2 h_2^2 5ih_4^2 5ih_2^2 6ih_4^2 6i}; \quad (3)$$
$$\hat{d}_1^{(1)} = r_1 h_2 3 i^2 h_1 4 i^2 : \quad (4)$$
$$\hat{d}_1^{(2)} = r_1 h_1 2 i^2 h_3 4 i^2 : \quad (5)$$
$$d_1(s_{23}; s_{34}; s_{561}) = 2 \frac{\binom{2}{2}}{s_{23}s_{34}} \frac{\hat{d}_1^{(1)} + \hat{d}_1^{(2)}}{2}; \quad (6)$$
$$r_{2B} = 8 \frac{h^3 p_{123}^2 j^2 h^6 p_{123}^2 j^2}{h^2 3ih^2 6ih^4 3ih^4 6i}; \quad (7)$$
$$\hat{d}_{2B}^{(1)} = r_{2B} \ln 6i^2 h3 5i^2 : \quad (8)$$
$$\hat{d}_{2B}^{(2)} = r_{2B} \ln 3 i^2 \ln 5 i^2 : \quad (9)$$
$$d_{2B}(s_{123}; s_{345}; s_{12}; s_{45}) = \frac{\binom{2}{s_{123}s_{345}} \binom{2}{s_{12}s_{45}}}{2} \frac{d_{2B}^{(1)} + d_{2B}^{(2)}}{2} : \quad (10)$$
$$I_{2A} = \frac{8 \overline{s_{345} s_{56}^2}}{h_2^2 g_1^3 s_3 h_6 p_{12}^2 h_2 p_{34}^2 h_6 p_{34} p_{12}^2 g_1^3 s_4 p_{12}^2}; \quad (11)$$
$$\hat{d}_{2A}^{(1)} = r_{2A} s_{345}^2 h_{61i}^2 [45]^2 : \quad (12)$$
$$\hat{d}_{2A}^{(2)} = r_{2A} h_1 p_{34} p_1^2 h_6 p_{12} p_4^2 \quad (13)$$
$$d_{2A}(s_{12}; s_{34}; s_{345}; s_{56}) = 2 \frac{\binom{2}{s_{345} s_{56}}}{s_{345} s_{56}} \frac{\hat{d}_{2A}^{(1)} + \hat{d}_{2A}^{(2)}}{2} \quad (14)$$
$$r_1 = 8 \frac{S_{45} S_{56} S_{456}}{h_4 6 i^2 h_4 P_{123} 1 h_4 P_{123} 3 h_6 P_{123} 1 h_6 P_{123} 3} ; \quad (15)$$

the result of the quadruple-cut $\hat{d}_1^{(1)}$ for the configuration displayed in Fig 2 is

$$\hat{d}_1^{(1)} = r_1 h_4 5i^2 h_6 \mathcal{P}_{123} \mathcal{P}_j^2 : \quad (16)$$

By reversing the internal helicities one gets

$$\hat{d}_1^{(2)} = r_1 h_5 6i^2 h_4 \mathcal{P}_{123} \mathcal{P}_j^2 : \quad (17)$$

The coefficient of $F_1(s_{45}; s_{56}; s_{123})$, the finite part of the one-mass box, reads

$$d_1(s_{45}; s_{56}; s_{123}) = 2 \frac{(-2)}{s_{45}s_{56}} \frac{\hat{d}_1^{(1)} + \hat{d}_1^{(2)}}{2} : \quad (18)$$

Three-mass Triangle $(1^+ 2^+ \beta^- 4^+ \bar{\beta}^- 6^+)$

From the triple-cut of the configuration displayed in Fig 2, the triangle coefficient reads

$$\hat{c}_3^{(1)} = 4 \frac{h_1 2ih_1 \mathcal{P}_{34} \mathcal{P}_j^2 e_1^2}{h_2 4ih_3 4i} \frac{N_{e_1}}{D_{e_1}} + \frac{n}{e_1!} \frac{o}{e_2!} ; \quad (19)$$

with

$$N_{e_1} = \begin{aligned} & h_1 s_{12} h_1 3i + (s_{12} - s_{34}) h_1 3i + h_1 \mathcal{P}_{34} \mathcal{P}_{12} \mathcal{P}_i e_1 \\ & h_1 s_{12} s_{34} h_1 5ie_1 + h_1 \mathcal{P}_{12} \mathcal{P}_{34} \mathcal{P}_i (s_{12} + (s_{12} - s_{34}) e_1) \\ & h_1 s_{12} h_1 3ih_2 4i + (s_{12} - s_{34}) h_1 3ih_2 4i \\ & + h_3 4ih_1 \mathcal{P}_{34} \mathcal{P}_{12} \mathcal{P}_i - h_3 2ih_1 \mathcal{P}_{34} \mathcal{P}_{12} \mathcal{P}_i e_1 ; \end{aligned} \quad (20)$$

$$D_{e_1} = \begin{aligned} & h_1 s_{12} h_1 2i + (s_{12} - s_{34}) h_1 2i + h_1 \mathcal{P}_{34} \mathcal{P}_{12} \mathcal{P}_i e_1 \\ & h_1 s_{12} s_{34} h_1 6ie_1 + h_1 \mathcal{P}_{12} \mathcal{P}_{34} \mathcal{P}_i (s_{12} + (s_{12} - s_{34}) e_1) \\ & h_1 s_{12} h_1 4i + (s_{12} - s_{34}) h_1 4i + h_1 \mathcal{P}_{34} \mathcal{P}_{12} \mathcal{P}_i e_1 \\ & h_1 s_{12} h_1 6i + (s_{12} - s_{34}) h_1 6i + h_1 \mathcal{P}_{34} \mathcal{P}_{12} \mathcal{P}_i e_1 \\ & h_1 s_{12} h_1 \mathcal{P}_{34} \mathcal{P}_i e_1 + h_1 \mathcal{P}_{12} \mathcal{P}_i (s_{12} + (s_{12} - s_{34}) e_1) \\ & h_1 s_{12} + s_{12} - s_{34} + h_1 \mathcal{P}_{34} \mathcal{P}_i e_1 ; \end{aligned} \quad (21)$$

where

$$e_{1,2} = \frac{s_{12}}{2} \frac{3s_{34} - s_{56} - s_{12}}{s_{12}(s_{34} - s_{56}) + s_{34}(-2s_{34} + s_{56})} ; \quad (22)$$

with

$$_{12;34;56} = s_{12}^2 + s_{34}^2 + s_{56}^2 - 2s_{12}s_{34} - 2s_{12}s_{56} - 2s_{34}s_{56} ; \quad (23)$$

The contribution coming from reversing the inner helicities, $\hat{c}_3^{(2)}$, amounts to the same value, $\hat{c}_3^{(2)} = \hat{c}_3^{(1)}$; therefore the coefficient of $I_3(s_{12}; s_{34}; s_{56})$, the three-mass triangle within the amplitude is,

$$c_3(s_{12}; s_{34}; s_{56}) = 2 (\hat{c}_3^{(1)} + \hat{c}_3^{(2)}) ; \quad (24)$$

where the factor 2 accounts for the contribution coming from a fermion looping in the opposite-direction. Although not manifest in Eqs.(20,21), one can see analytically that in (19) the dependence on \mathcal{P}_j drops out, because e_1 and e_2 only differ in the sign of \mathcal{P}_j . Therefore c_3 is a rational function of spinor products.

3. Form factor approach

In the Feynman-diagrammatic approach the six-photon amplitude is represented by 120 one-loop diagrams which differ only by permutations of the external photons.

As the corresponding integrals are IR/UV finite, the Dirac algebra can be performed in $D = 4$ dimensions. However, using algebraic tensor reduction, one has to work with a $(4 - 2\epsilon)$ -dimensional loop momentum, since at intermediate steps scalar integrals are generated which are formally divergent in $D = 4$ dimensions. The respective coefficients will drop out in the end, which serves as a check of the computation. We use the spinor helicity method and define projectors on the helicity amplitudes $A_6(++++)$ and $A_6(+-++)$ in such a way that (by choosing convenient reference momenta for the polarisation vectors) we obtain global spinorial factors for each amplitude. The resulting expressions contain integrals with scalar products of external vectors and loop momenta in the numerator. For the six-point integrals all scalar products between the loop momentum and external momenta are reducible, i.e. they can be written as differences of inverse propagators. As a result, at most rank-one six-point functions have to be evaluated. For the $(N < 6)$ -point functions at most three loop momenta remain in the numerator. As was shown in [27], this can be related to the cut-constructibility argument of [31]. To reduce the irreducible tensor integrals to scalar integrals we use the algebraic approach outlined in [6], which leads to a representation of the amplitude in terms of the basis functions $I_3; F_1; F_{2A}; F_{2B}$. The formalism is implemented using FORM [35]. The coefficients of the basis functions are then stored and simplified further with Maple and/or Mathematica. The same setup was already used for simpler 4- and 5-point loop amplitudes [34].

Although only a restricted set of functions actually needs to be evaluated due to the symmetry properties of the amplitude, the symmetry relations serve as a stringent check on the implementation. Therefore, and in order to test our setup in view of future applications, all 120 diagrams have been calculated.

We stress that the resulting expressions for the coefficients, although they are not evaluated in terms of spinor products, allow for a fast numerical evaluation. We note that in all expressions at most one power of inverse Gram determinants survives, which is intrinsic to the chosen function basis.

We have cross-checked the result obtained by the form factor approach with the one achieved by using the cutting rules and find perfect agreement. We have further compared to the recent numerical result of Nagy and Soper [20]: mapping our helicity configuration onto their one, according to $A_6(2^-; 1^+; 3^-; 4^+; 5^-; 6^+) = A_6(1^+; 2^-; 3^-; 4^+; 5^+; 6^-)$; and using the same kinematics as in Fig. 5 of [20], we find the result shown in Fig. 3, which agrees with Nagy and Soper. We note that our results are produced by simply evaluating the analytical expressions obtained by the form factor approach, therefore we do not have numerical errors.

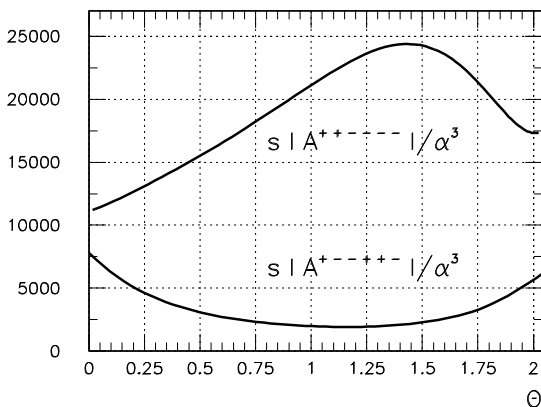


Figure 3. The modulus of the normalised six-photon helicity amplitudes $s | \mathcal{A}_6(++) \rangle \frac{1}{\alpha^3}$ and $s | \mathcal{A}_6(+ +) \rangle \frac{1}{\alpha^3}$ plotted for the kinematics as defined in [20].

4. Conclusions

The six-photon amplitudes can be fully expressed as linear combinations of known one-loop master integrals with three and four external momenta. Using the techniques of form factor decomposition [6] and of multiple cuts [11, 12, 13, 14], we have derived analytic expressions for the coefficients of the master integrals. The expressions obtained from the multiple-cut method are typically more compact than the form factor results, such that we decided to quote only the former. All coefficients agree numerically. We fully confirm earlier purely numerical results [20] for the six-photon amplitudes. Our calculation demonstrates the applicability of the form factor decomposition and multiple-cut methods to non-trivial multi-leg processes at one-loop, and illustrates that both methods can be formulated in the same integral basis. In future applications, one could therefore envisage to combine both methods. Our result shows that the analytical evaluation of one-loop amplitudes with similar kinematics relevant for the LHC is feasible.

Acknowledgements

We would like to thank Jean-Philippe Guillet, Christian Schubert and Daniel Egli for collaboration during early stages; Simon Badger, Ruth Britto and Andrea Ferroglia, for clarifying discussions. GH would like to thank the ITP at Zurich University for its hospitality. This research was supported in part by Marie-Curie-EIF under contract MEIF-CT-2006-024178, by the Swiss National Science Foundation (SNF) under contract 200020-109162, the UK Particle Physics and Astronomy Research Council (PPARC) and the Scottish Universities Physics Alliance (SUPA).

REFERENCES

1. R. Karplus and M. Neumann, Phys. Rev. 80 (1950) 380; 83 (1951) 776; B. De Tollis, Nuovo Cim. 32 (1964) 757, 35 (1965) 1182.
2. Z. Bern, et al., JHEP 0111 (2001) 031.
3. T. Binoth, et al., JHEP 0205 (2002) 060.
4. C. Anastasiou, et al., Phys. Rev. Lett. 91 (2003) 251602.
5. Z. Bern, et al., arXiv:hep-th/0610248.
6. T. Binoth, et al., JHEP 0510 (2005) 015; Nucl. Phys. B 572 (2000) 361.
7. C. F. Berger, et al., Phys. Rev. D 74 (2006) 036009.
8. R. K. Ellis, et al., Phys. Rev. D 73 (2006) 014027.

9. A. Denner, S. Dittmaier, Nucl. Phys. B 734 (2006) 62.
10. C. Anastasiou and A. Daleo, JHEP 0610 (2006) 031.
11. R. Britto, et al., Nucl. Phys. B 725, (2005) 275.
12. R. Britto, et al., Phys. Rev. D 72, (2005) 065012.
13. R. Britto, et al., Phys. Rev. D 73, (2006) 105004.
14. P. Mastrolia, Phys. Lett. B 644 (2007) 272.
15. C. Anastasiou, et al., Phys. Lett. B 645 (2007) 213;
arXiv:hep-ph/0612277.
16. R. Britto and B. Feng, arXiv:hep-ph/0612089.
17. A. Brandhuber, et al., JHEP 0510 (2005) 011.
18. G. Ossola, et al., Nucl. Phys. B 763 (2007) 147.
19. Z. Xiao, et al., Nucl. Phys. B 758 (2006) 53.
20. Z. Nagy and D. E. Soper, Phys. Rev. D 74 (2006)
093006.
21. R. K. Ellis, et al., JHEP 0605 (2006) 027.
22. A. Denner, et al., Nucl. Phys. B 724 (2005) 247.
23. A. Lazopoulos, et al., arXiv:hep-ph/0703273.
24. C. Anastasiou, et al., arXiv:hep-ph/0703282.
25. G. Mahlon, Phys. Rev. D 49 (1994) 2197.
26. G. Mahlon, in proceedings of Beyond the Standard
Model IV, eds. J. Gunion, T. Han, J. Ohnishi, World
Scientific (River Edge NJ, 1995).
27. T. Binoth, et al., JHEP 0702 (2007) 013.
28. G. 't Hooft, and M. Veltman, Nucl. Phys. B 153
(1979) 365.
29. Z. Bern, et al., Phys. Lett. B 302 (1993) 299
[Erratum -ibid. B 318 (1993) 649];
Nucl. Phys. B 412 (1994) 751.
30. T. Binoth, et al., Nucl. Phys. B 615 (2001) 385.
31. Z. Bern, et al., Nucl. Phys. B 425 (1994) 217; Nucl.
Phys. B 435 (1995) 59.
32. K. J. Ozeren, W. J. Stirling, JHEP 0511 (2005) 016.
33. D. Maître and P. Mastrolia, in preparation.
34. T. Binoth, et al., JHEP 0612 (2006) 046; JHEP 0503
(2005) 065; JHEP 0402 (2004) 057.
35. J. A. M. Vermaseren, arXiv:math-ph/0010025.